Isolation and characterization of cellulose from coconut shell powder and its application as reinforcement in casein composite films

Adarsh M. Kalla (adarshkalla002@gmail.com)
National Dairy Research Institute
Magdaline Eljeeva
National Dairy Research Institute
Heartwin A. Pushpadass
National Dairy Research Institute
Sathish Kumar
National Dairy Research Institute
Surendra Nath Battula
National Dairy Research Institute

Research Article

Keywords: casein composite film, cellulose, characterization, coconut shell powder, film properties

Posted Date: August 24th, 2022

DOI: https://doi.org/10.21203/rs.3.rs-1960474/v1

Isolation and characterization of cellulose from coconut shell powder and its application as reinforcement in casein composite films

Adarsh M. Kalla[a], Magdaline Eljeeva Emerald Franklin [a,*], Heartwin A. Pushpadass[a], Sathish Kumar M.H.[a] and Surendra Nath Battula[a]

[a]*Southern Regional Station, ICAR-National Dairy Research Institute, Bengaluru, India*

Corresponding author: Email: adarshkalla002@gmail.com, orcid.org/0000-0002-5981-4645

Abstract

Cellulose was extracted from coconut shell powder (CSP) as a source of natural fiber, and used as reinforcing material in casein composite films. Extraction was done by delignification and mercerization of CSP, with yield of 27.5% cellulose. The isolated cellulose was characterized by scanning electron microscopy (SEM), atomic force microscopy (AFM), X-ray diffractometry (XRD) and Fourier transform infrared spectroscopy (FTIR). The SEM micrographs revealed that the mean width of microfibrils was 5-20 µm, while AFM showed mean surface roughness of 1.37 nm. FTIR spectra revealed the absence of lignin and hemicellulose in the cellulose, indicating their successful removal from CSP during extraction of cellulose. XRD indicated crystallinity content of 65.4% in cellulose. The flow properties of extracted cellulose were compared with that of commercial grade cellulose. The bulk, tapped and true densities of extracted cellulose were 368.8, 493.8 and 1313 kg/m^3, respectively, whereas Hausner ratio and Carr's index were 1.34 and 25.3%, respectively. The reinforcing capacity of 3% cellulose was evaluated in casein films prepared by casting. Casein composite films with added cellulose increased their tensile strength and elastic modulus from 4.98 to 7.20 MPa and 9.91 to 83.42 MPa, respectively. However, the tensile strain decreased from 52.08 to 8.66% after incorporation of cellulose, indicating good toughness and resistance to deformation.

KEYWORDS: casein composite film, cellulose, characterization, coconut shell powder, film properties

1. Introduction

Natural fibers used as fillers/reinforcements in composite films has increased tremendously in recent times as they are environment friendly and shown to improve the film properties (Satyanarayana, Arizaga, & Wypych, 2009). Apart from being biodegradable, the natural fibers are cost effective and renewable, possess low density, high tensile strength and release negligible CO_2 emissions. The natural fiber-reinforced composites are not a suitable replacement for synthetic polymers in every packaging application because of their limitations such as poor compatibility with other polymer matrices and hydrophilicity in composites but can be used as single-use packaging material (John & Anandjiwala, 2008; Deka, Misra, & Mohanty, 2013; Majeed et al., 2013). Adhesion of natural fibers with other polymer matrices could be improved and their moisture uptake could be reduced through chemical treatments such as benzoylation, acetylation, acrylation, alkalization and silane treatment. These treatments modify the hydroxyl groups in natural fibers that impart hydrophilicity (John & Anandjiwala, 2008).

Natural fibers obtained from plant and cellulose-based sources are common bio-fillers for reinforcing polymer matrices (Singha & Thakur, 2009). Notably, quality fibrous fillers can be obtained from agricultural wastes such as bagasse, wheat straws, rice husks, groundnut shells, coconut husk and cotton stalks (Thakur, Thakur, & Gupta, 2014). Wood and cotton are the principal sources for cellulose, a natural fiber. Coconut shell contains lignin, hemicellulose and cellulose, which possess good thermo-stability (Mantia, Morreale, & Ishak, 2005). It is available in abundance in the tropical countries, wherein 90% of them are disposed as waste, used as fuel or burnt in open air (Madakson, Yawas, & Apasi, 2012). Cellulose could be extracted from

agricultural wastes such as coconut shell by removing the non-cellulosic constituents by delignification and mercerization. Hence, coconut shell powder (CSP) can be a good source for obtaining cellulosic fibers for manufacturing of composites (Sarki, Hassan, Aigbodion, & Oghenevweta, 2011).

Cellulose is a straight chain semi-crystalline polymer of D-glucopyranose units with no branching of the molecular chains. In most agricultural sources, it is available as a composite material along with other components as lignocellulose, hemicellulose, etc. The chemical structure of cellulose is similar to that of starch. However, due to the β(1→4) glycosidic bonds that exist within, cellulose makes it extremely rigid. Each unit of cellulose contains three hydroxyl groups associated with hydrogen bonds to form bundles of fibrils, wherein highly ordered crystalline regions alternate with disordered amorphous regions (Bodirlau, Teaca, & Spiridon, 2013). Due to its fibrous nature, cellulose as a bio-filler can align and orient itself uniaxially enhancing its mechanical strength (Haafiz et al., 2013), flexibility, biocompatibility, thermal and chemical stability (Hahary, Husseinsyah, & Zakaria, 2016). The utilization of cellulose as reinforcement in thermoplastic matrices was demonstrated by several researchers (Haafiz et al., 2013; Teacă, Bodîrlău, & Spiridon, 2013; Hahary et al., 2016; Sudharsan et al., 2016). Similarly, addition of 15% (w/w) cellulose to starch-based films improved their water resistance (Dufresne & Vignon, 1998).

Casein is a unique milk protein with random coil structure, and possess excellent film-forming properties due to the lack of secondary structure and presence of weak intermolecular electrostatic, hydrophobic and hydrogen bond interactions (McHugh & Krohta, 1994). It tends to

77 form transparent and flexible films because the presence of hydroxyl and amino groups in casein
78 provides good oxygen barrier property to the films (Bonnaillie, Zhang, Akkurt, Yam, &
79 Tomasula, 2014). Since casein has polar groups, it can be used in combination with other
80 polymers (fat based polymers) in order to protect products that are prone to oxidation. However,
81 due to the presence of hydrophilic groups, these films have poor mechanical and moisture barrier
82 properties, which could be circumvented to a large extent by incorporation of cellulosic fibers as
83 reinforcing agent.
84
85 This study aims to produce packaging films from natural biopolymers such as casein and
86 cellulose. Cellulose was extracted from CSP as there have been few attempts to extract it from
87 this cheap source. The objective was to improve the mechanical and water vapor barrier
88 properties of casein films by incorporation of cellulose fibers extracted from CSP. The
89 improvement in mechanical and water vapor barrier properties of casein films after
90 reinforcement with cellulosic fibers was evaluated.
91
92 **2. Experimental Methods**
93 *2.1. Materials*
94 CSP was provided by Master Micron International (Bengaluru, India), while sodium
95 chlorite (83%, MW: 90.44), glacial acetic acid (99.6%, MW: 60.05) and sodium hydroxide
96 (97%) were purchased from HiMedia Laboratories Pvt. Ltd. (Mumbai, India). All other
97 chemicals used were of analytical reagent grade.
98
99

100 *2.2. Extraction of cellulose fibers*

101 The CSP was sieved using sieve shaker (Model: Retsch AS 200, Germany) to ≤63 μm for
102 extraction of cellulose. The extraction and removal of non-cellulosic components from CSP was
103 done by delignification and mercerization. Delignification was performed in accordance with
104 ASTM D1104-56 (1978) to primarily remove lignin. The CSP was washed with warm water at
105 50°C to remove the impurities, and dried at 70°C for 2 h. It was bleached by acidified sodium
106 chlorite solution, with pH adjusted to 3-4 by glacial acetic acid at 70°C for 5 h to remove lignin.
107 The cellulose obtained was referred to as 'holocellulose', which was filtered, washed and rinsed
108 with distilled water. The holocellulose was further treated with aqueous solution of 5% NaOH
109 for 2 h at ambient temperature to produce cellulose according to ASTM D1103-60 (1977). The
110 solution was filtered, washed with distilled water and oven-dried at 70°C for 8 h. The cellulose
111 yield was expressed as percentage of CSP used (Eq. 1).

112 $$\text{Yield (\%)} = \frac{W_f}{W_i} \times 100 \quad (1)$$

113 where, 'W_i' is the initial weight of CSP and 'W_f' is the final dried weight of extracted cellulose.

114

115 *2.3. Moisture content*

116 Exactly 3 g of CSP was spread in a Petri plate and oven-dried at 105ºC for 24 h. (Ilyas,
117 Sapuan, & Ishak, 2017). It was transferred to a desiccator, cooled and weighed to estimate the
118 moisture content (Eq. 2). The moisture contents of extracted and commercial celluloses were
119 similarly estimated.

120 $$\text{Moisture content} = \frac{M_i - M_f}{M_i} \times 100 \quad (2)$$

121 where, 'M_i' is the initial weight of sample and 'M_f' is the final dried weight.

122 *2.4. Optical microscopy*

123 The structure of CSP, extracted cellulose and commercial cellulose was observed using
124 an optical microscope (Model: Nikon YS200, Minato, Tokyo, Japan). A drop of suspension
125 prepared using distilled water was spread on the glass slide, stained with methylene blue to
126 obtain adequate contrast, and images were acquired at 100X and 400X magnifications.

127

128 *2.5. Scanning electron microscopy-energy dispersive X-ray spectroscopy*

129 The morphology of extracted and commercial celluloses was examined by scanning
130 electron microscopy (SEM) (Model: Ultra 55, Zeiss, Jena, Germany). The samples were sputter-
131 coated with 5-10 nm gold to make them conductive, and were observed under 10^{-5} mbar vacuum
132 with accelerating voltage of 5 kV. Energy dispersive X-ray spectroscopy (EDS) was used to
133 identify the elemental composition of celluloses. The detector used was X-Max EDS (Oxford
134 Instruments, Oxford, UK) with Peltier cooling.

135

136 *2.6. Atomic force microscopy*

137 The morphology and surface roughness of cellulose extracted from CSP was determined
138 using atomic force microscope (AFM) (Model: ScanAsyst, Bruker, Santa Barbara, USA).
139 Samples were prepared by dispersing 100 mg of cellulose in 10 mL deionized water, and the
140 mixture was ultrasonicated for 8-10 min. Exactly 20 µL of the mixture was drop-casted on a
141 clean slide and dried for 36 h under vacuum. The morphology and topography of cellulose were
142 analyzed using 2-D and 3-D images.

143

144 *2.7. X-ray diffractometry*

145 The X-ray diffraction (XRD) was used to examine the crystallinity of CSP and both
146 celluloses. The samples were analyzed in the X-ray diffractometer (Model: Rigaku SmartLab,
147 Tokyo, Japan) using Cu-Kα radiation (λ=0.154 nm) at 40 kV and 30 mA with goniometer speed
148 of 0.02 s^{-1}. The spectra were measured for 2θ in the range of 10-40°. The X-ray detector used
149 was scintillation counter, with detector angle of 40º, and placed at a distance of 300 mm. The
150 crystallinity index was calculated using Eq. (3) as suggested by Segal, Creely, Martin Jr, and
151 Conrad (1959).

152 $$\text{Crystallinity index} = \frac{I_{002} - I_{am}}{I_{002}} \times 100 \quad (3)$$

153 where, 'I_{002}' (002 plane diffraction) is the peak intensity of the crystalline regions and 'I_{am}' is the
154 peak intensity of amorphous region.
155
156 *2.8. Fourier transform infrared spectroscopy*
157 The Fourier transform infrared (FTIR) spectra of CSP and celluloses were recorded using
158 the FTIR spectrometer (Model: Perkin Elmer Frontier, Singapore). The sample was finely
159 ground, mixed with potassium bromide in the ratio of 5:95 and compressed into pellets using 5
160 tonne press. The wavenumber of the scans varied from 400 to 4000 cm^{-1} with 32 scans per
161 minute at the spectral resolution of 4 cm^{-1}.
162
163 *2.9. True density*
164 The true density (ρ_{true}) was calculated using the method given by Pushpadass, Emerald,
165 Rao, Nath, and Chaturvedi (2014) Exactly 5 g of sample was taken in 50 mL centrifuge tube and
166 25 mL of petroleum ether was added to it. The tube was closed with an air-tight stopper. The
167 sample contained in the tube was vortexed for 1 minute to ensure that all particles

were evenly dispersed. Again 3 mL of petroleum ether was used to wash the powder particles sticking to the walls of the tube, and the contents were vortexed for 5 min. The total volume of petroleum ether along with suspended powder was read, and true density was calculated using Eq. (4).

$$\text{True density } (\rho_{true}) = \frac{\text{Weight of powder (g)}}{\text{Total volume of petroleum ether with suspended powder (mL) - 28}} \quad (4)$$

2.10. Flow properties

The bulk and tapped densities of CSP and celluloses were determined as per the method given by Mitra et al. (2017) Briefly, 50 g of sample (W) was allowed to flow freely through a funnel into 250 mL graduated cylinder, and it was gently tapped on a wooden bench three times. The bulk volume (V_o) was recorded, and the bulk density (ρ_{bulk}) was computed using Eq. (5). For tapped density (ρ_{tapped}), the cylinder with sample was tapped 500 times using the tapped density tester (Model: Thermonik, Campbell Electronics, Mumbai, India), and the final tapped volume was recorded (V_f). The tapped density was determined using Eq. (6).

$$\text{Bulk density } (\rho_{bulk}) = \frac{W}{V_0} \quad (5)$$

$$\text{Tapped density } (\rho_{tapped}) = \frac{W}{V_f} \quad (6)$$

The Carr's index (CI) and Hausner ratio (HR) indicate the flowability and cohesiveness of powders. The CI and HR of CSP and celluloses were calculated from ρ_{bulk} and ρ_{tapped} using Eqs. (7) and (8), respectively.

$$\text{Carr's index (\%)} = \frac{\rho_{tapped} - \rho_{bulk}}{\rho_{tapped}} \times 100 \quad (7)$$

$$\text{Hausner ratio} = \frac{\rho_{tapped}}{\rho_{bulk}} \quad (8)$$

The porosity of CSP and celluloses was estimated from the ρ_{bulk} and ρ_{true} using Eq. (9).

$$\text{Porosity (\%)} = \left(1 - \frac{\rho_{bulk}}{\rho_{true}}\right) \times 100 \quad (9)$$

The static angle of repose (AoR) was measured using optical imaging method. Both cellulose powders were allowed to pass through a fixed funnel to form a free-standing pile on a plane surface. The images of the sample pile were captured using a digital camera. The AoR was computed from the images using the "DropSnake" plugin of ImageJ software ver. 1.45 (National Institutes of Health, Bethesda, MD) after converting them into gray-scale (Mitra et al., 2017).

2.11. Reinforcing ability of isolated cellulose fibers

The reinforcing capacity of extracted cellulose was assessed in casein films prepared by casting (Wagh, Pushpadass, Emerald, & Nath, 2014). The film forming solution was prepared by dissolving 18 g of casein in 200 mL of warm distilled water, whose pH was adjusted to 5.6 using 2 N NaOH solution. The cellulose was added as reinforcing agent at 3%, maintaining the total solids content in the film-forming solution at 9%. The solution was heated on a hot plate at 85ºC with constant stirring for 15 min. Glycerol was added as plasticizer at 0.25% (w/w) of solution, while potassium sorbate at 0.2% (w/w) of biopolymer was added as antimicrobial agent. Heating was continued for 5 min and the solution was cooled to 40-45ºC, and poured onto glass molds of

290×200×4 mm size lined with polytetrafluoroethylene (PTFE) sheet. The film-forming solutions were dried at 40ºC for 96 h. After drying, the films were peeled-off from the molds and equilibrated at 27ºC and 65% RH for 48 h in a desiccator containing saturated potassium iodide solution before testing.

The thickness of cast films was measured using a digital caliper (Model: CD 6"CSX, Mitutoyo Corp., Japan) at 5 random locations and the mean value was calculated. The water vapor permeability (WVP) of the films was determined using water vapor transmission rate (WVTR) estimated gravimetrically using wet cup method (ASTM E96-95, 1995). The film specimen of 8×8 cm was cut and mounted on polycarbonate cups filled with distilled water to 1 cm from the film underside. The lid was tightened and cup with film was then placed in stability chamber maintained at 27°C and 65% RH. The weight loss of the cup was measured at 2 h interval and the steady state portion of the weight loss (up to 12 h) versus time curve was used to compute the WVTR. The WVP was computed using Eq. (10).

$$WVP = \frac{WVTR \times t}{\Delta p} \tag{10}$$

where, 't' is mean thickness of film specimen and 'Δp' is water vapor partial pressure difference (kPa) between the two sides of specimen. Each film was analyzed three times and the mean WVP was computed.

The tensile properties of the films were analyzed using the texture analyzer (Model: TA.XT Plus, Stable Micro Systems, Godalming, Surrey, UK). Strips of 2.5×15 cm were cut, and were fixed onto the jaws of A/TG tensile grips. The distance between the grips was kept at 100

231 mm, and the film strips were tested at the speed of 0.5 mm/s until they break. Tensile strength,
232 Young's modulus and elongation at break were determined with eight replications.
233
234 **3. Results and Discussion**
235 *3.1. Extraction and yield of cellulose*
236 The CSP obtained after sieving had a particle size of ≤63 μm, and was dark brown in
237 color due to the presence of hemicellulose and lignin. The progressive removal of hemicellulose
238 or lignin and consequent increase in cellulose content of CSP can be judged by the change in
239 color after each successive treatment (Fig. 1). Delignification changed the color of CSP from
240 dark brown to off white as lignin was removed. Further alkali treatment showed more evident
241 color change, and the powder exhibited the characteristic whiteness of cellulose. From the color
242 changes, it is evident that delignification was effective in removing non-cellulosic components
243 such as lignin, hemicellulose and waxes from CSP. After delignification and alkali treatment
244 (mercerization), about 30% of lignin and 42.5% of hemicellulose were removed, and the final
245 cellulose yield was about 27.5% of the initial weight of CSP. The results obtained were in
246 agreement with the yield of cellulose reported by Liyanage and Pieris (2015).

Coconut shell powder | Sieved coconut shell powder | Coconut shell powder after de-lignification | Cellulose extracted after de-lignification and mercerization

247
248 **Fig. 1** Cellulose extracted from coconut shell powder
249

3.2. Moisture content

The moisture content of cellulose fibers is an important characteristic while selecting it as filler in polymer composite films. Fiber with lower moisture content would be preferable as filler in bio-composites because higher moisture could reduce the tensile strength and lead to pore formation in the films (Razali, Salit, Jawaid, Ishak, & Lazim, 2015; Jumaidin, Sapuan, Jawaid, Ishak, & Sahari, 2017). The moisture content of CSP was 4.9%, while it was much less at 2.5% and 3.7% for extracted and commercial cellulose, respectively.

3.3. Optical microscopy

The particle size of CSP reduced considerably after sieving as seen from the light microscopic images (Figs. 2a and b). The cellulose fibers obtained after chemical treatment decreased in diameter because they became fibrillated due to the disruption of internal structure of CSP when non-cellulosic materials were removed by delignification and mercerization. Collazo-Bigliardi, Ortega-Toro, and Boix (2018) also observed similar reduction in diameter of cellulose extracted from coffee and rice husk after chemical treatment.

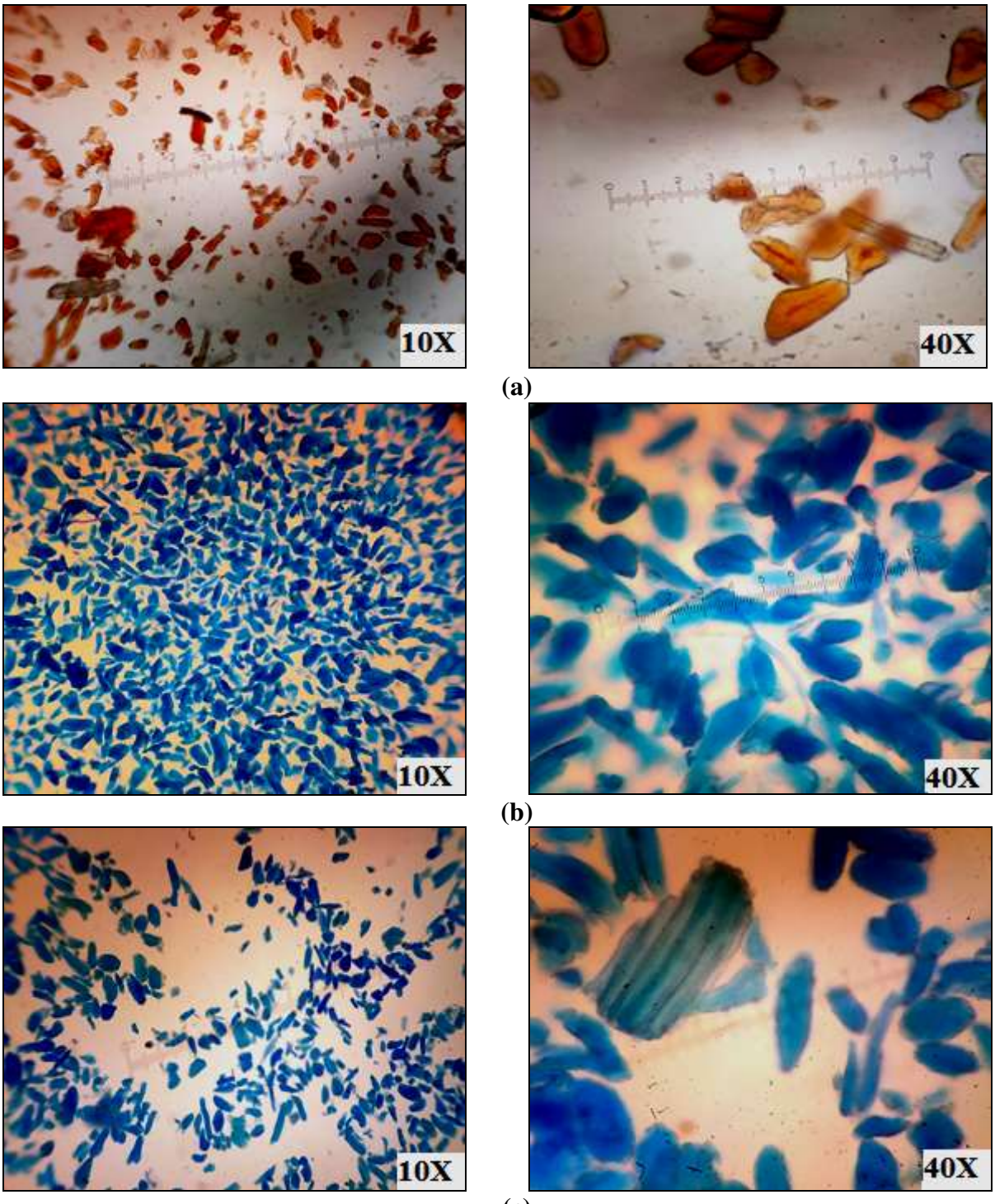

269 **Fig. 2** Optical microscopic images of (a) coconut shell powder (b) extracted cellulose and (c)

270 commercial cellulose

271

3.4. Scanning electron microscopy

. The SEM micrographs showed that the chemical treatment during extraction reduced the size of cellulose fibers from 63 µm to 5-20 µm (Fig. 3). The diameter of CSP reduced because the composite fibril structure was broken into individual cellulose micro-fibrils after the removal of lignin and hemicellulose. The empty space between the fibers (Fig. 3a) was indicative of the removal of non-cellulosic materials such as lignin, hemicellulose and waxes. The SEM image of commercial cellulose (Fig. 3b) also shows the presence of fibers in it. The diameter of cellulose obtained from CSP was similar in size to the cellulosic fibers of banana (10 µm) (Deepa et al., 2011), kneaf (13 µm) (Tawakkal, Talib, Abdan, & Ling, 2012), hibiscus sabdariffa (10.4 µm) (Sonia & Dasan, 2014), and oat husk (10-45 µm) (Qazanfarzadeh & Kadivar, 2016).

The EDS spectrum of both extracted and commercial cellulose showed the peaks of carbon, oxygen and nitrogen, and their elemental composition as well (Fig. 4). The carbon and oxygen content were to the extent of 34.84% and 46.08%, respectively The extracted cellulose also contained small amounts of impurities such as sodium at 0.54% and chlorine at 0.42%.

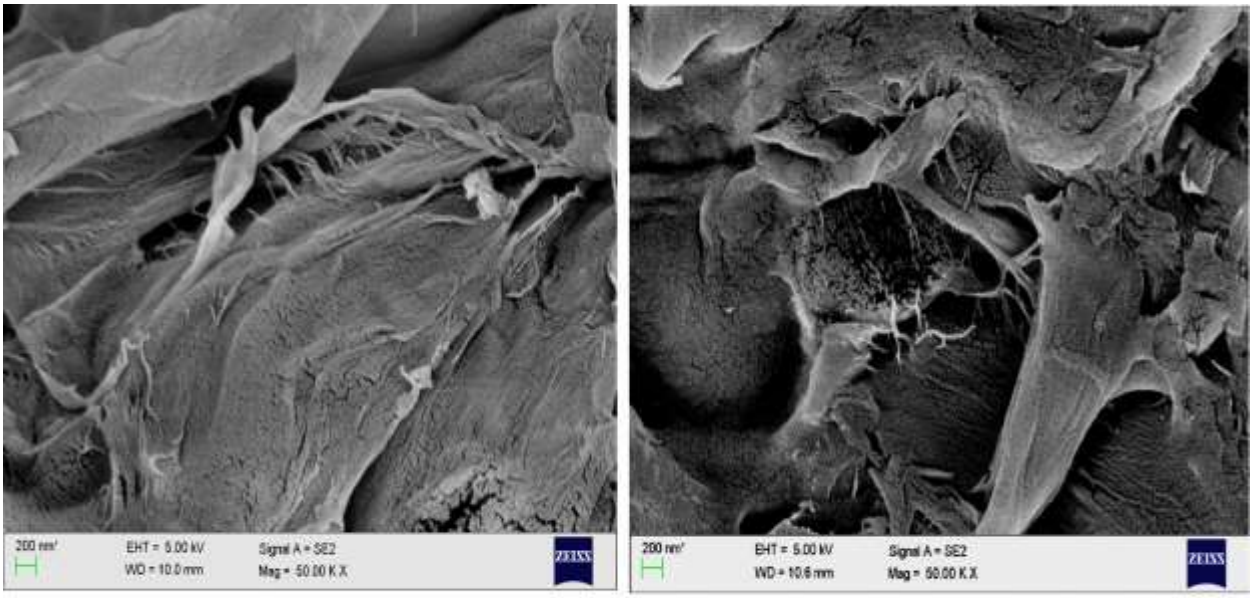

Fig. 3 Scanning electron micrographs of (a) cellulose extracted from CSP and (b) commercial cellulose microfibrils

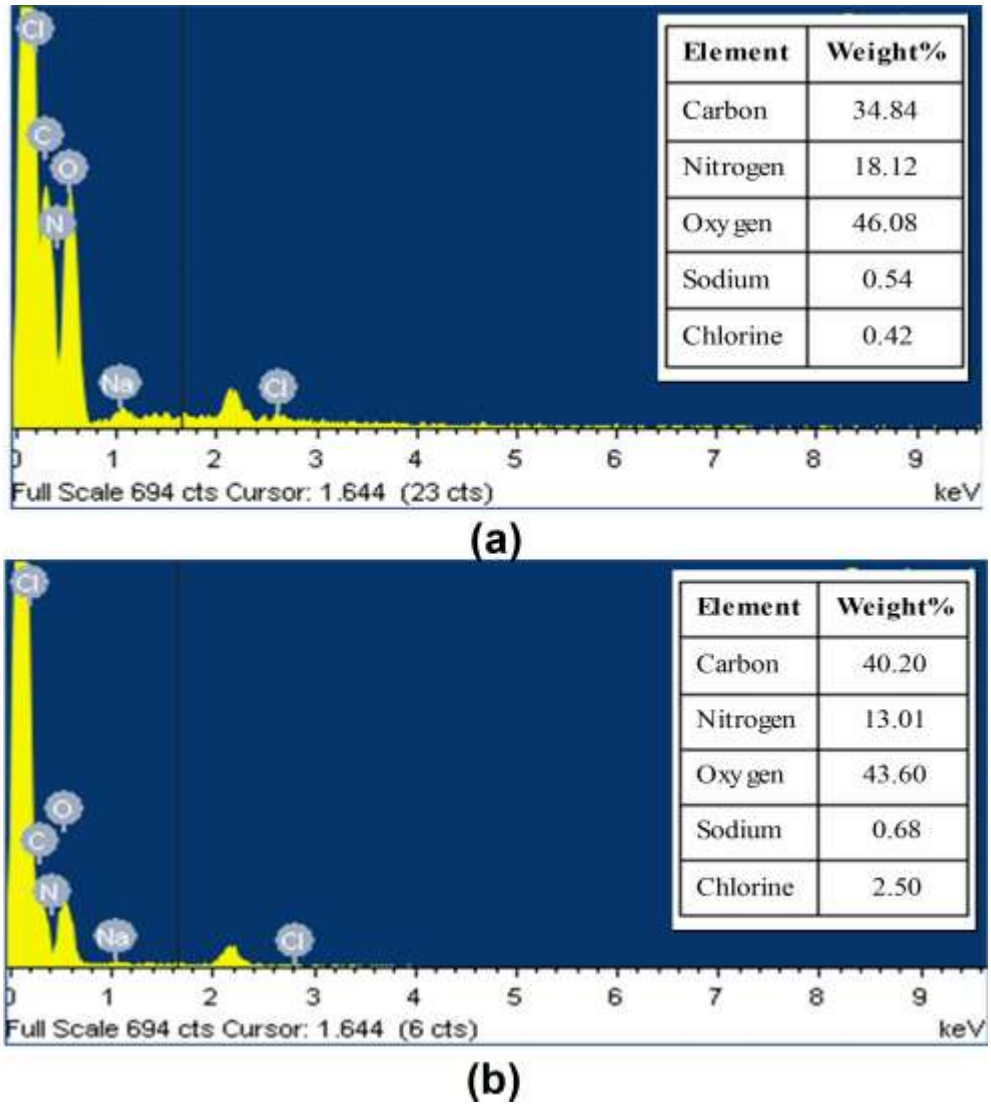

Fig. 4 Energy dispersive X-ray spectrum of (a) extracted cellulose and (b) commercial cellulose

3.5. Atomic force microscopy

The AFM topography of cellulose extracted from CSP is depicted in Fig. 5. The 2D image (Fig. 5a) shows aggregated structures with high surface area, which would support better interaction between casein and cellulose during processing into composite films. The 3D image (Fig. 5b) of extracted cellulose consisted of spherical particles with non-uniform and rough surfaces, with mean surface roughness of 1.37 nm. From Fig. 5a, it can be observed that

cellulose contained both brighter and darker regions, representing crystalline and amorphous regions, respectively.

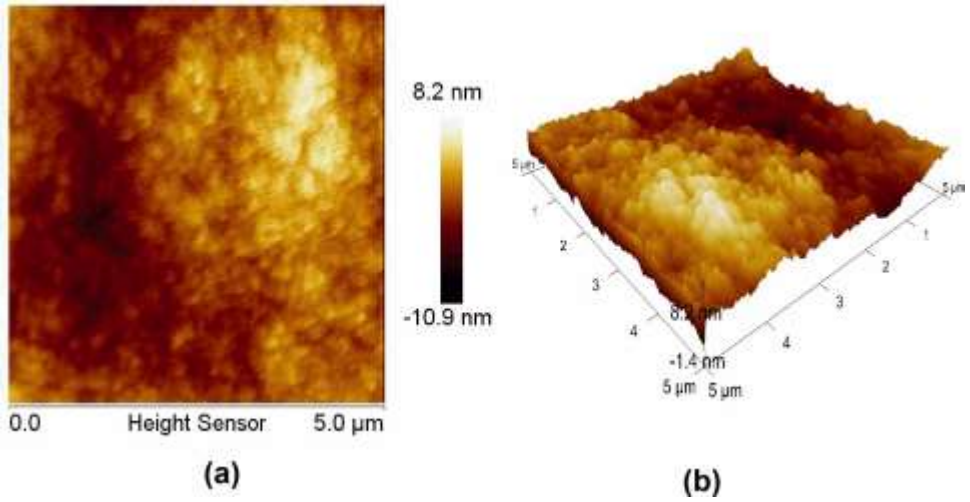

Fig. 5 2D (a) and 3D (b) atomic force microscopic images of extracted cellulose

3.6. X-ray diffractometry

Crystallinity is an important property that influences the mechanical properties of fibers. The X-ray diffractograms of CSP, extracted and commercial celluloses are shown in Fig. 6. The diffractograms (Fig. 6) of CSP, extracted and commercial celluloses displayed sharp peaks (I_{002}) at 2θ of 22.10º, 22.48º and 22.47º, respectively. The steep and intense I_{002} peak of extracted and commercial celluloses was typical of their higher crystalline content. The shoulder peak (I_{am}) of CSP, extracted cellulose and commercial cellulose was observed at 2θ of 16.46º, 17.82º and 18.35º, respectively. This indicated the dissolution of lignin and hemicellulose during chemical treatment. After non-cellulosic components were removed by delignification and mercerization, the crystallinity index noticeably increased from 47.8% in CSP to 65.9% in extracted cellulose. In comparison, commercial cellulose had much higher crystallinity index of 77.7%. The reduction in crystalline content in extracted cellulose and the additional peaks observed in the diffractogram were due to the ability of fibrils to rearrange themselves into less dense and rigid

interfibrillar regions and develop newer crystalline regions (Gassan & Bledzki, 1999). Sofla, Brown, Tsuzuki, and Rainey (2016) reported crystallinity index of 65% for cellulose extracted from bagasse.

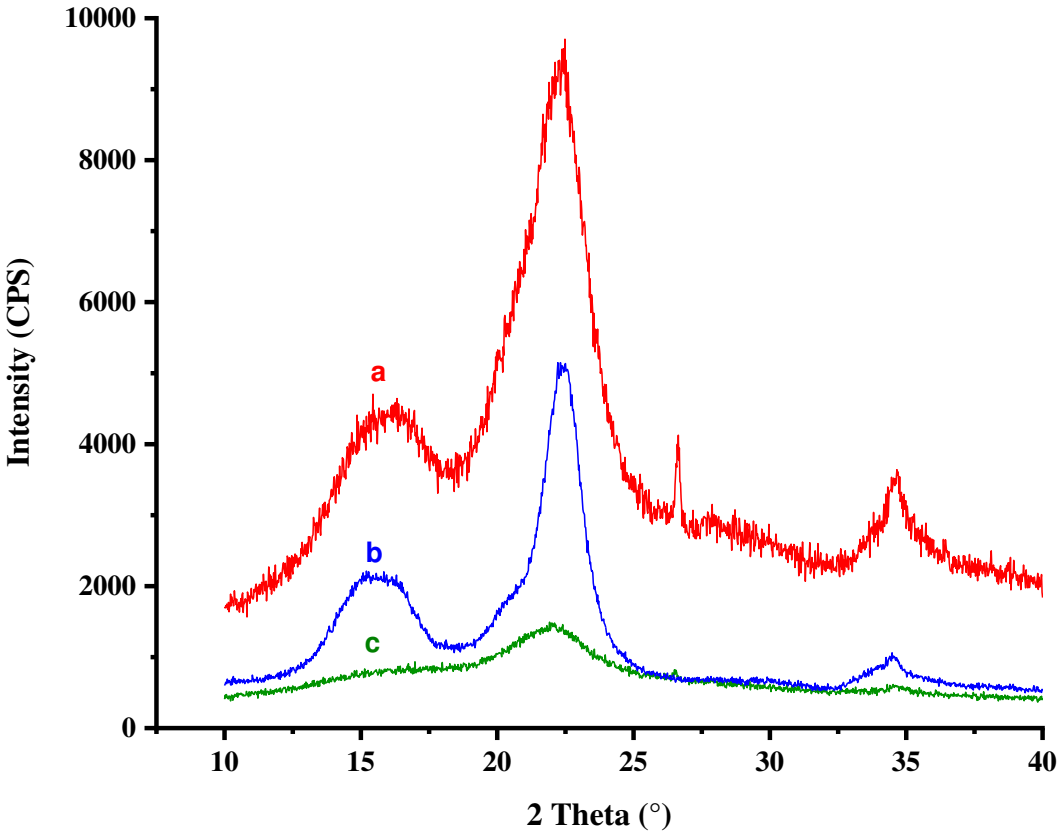

Fig. 6 X-ray diffraction patterns of (a) extracted cellulose (b) commercial cellulose and (c) coconut shell powder

3.7. Fourier transform infrared spectroscopy

The FTIR spectra of CSP, extracted and commercial celluloses are shown in Fig. 7 & 8 and Table 1. The typical bands of raw CSP were observed at 1740, 1608, 1511, 1458, 1247 and 1119 and 1010 cm^{-1}. In these, the bands at 1458 and 1247 cm^{-1} were due to lignin. The peaks at 1608 and 1511 cm^{-1} represented the C=C stretching vibrations of the aromatic ring of lignin (Qazanfarzadeh & Kadivar, 2016), while the peak at 1458 cm^{-1} was assigned to CH_3 bending and

330 at 1247 cm^{-1} was ascribed to C=O out-of-plane stretching vibrations of aryl group. These peaks
331 completely disappeared in extracted cellulose after chemical treatment (also absent in
332 commercial cellulose), indicating successful removal of lignin from the fibers. The band
333 observed at 1740 cm^{-1} in CSP was ascribed to C=O stretching of acetyl and uronic ester groups
334 of hemicellulose. The absence of this band in extracted and commercial celluloses also
335 corroborates the removal of hemicellulose by chemical treatment.
336
337 The broad absorption peak in the 3400-3100 cm^{-1} region, representing O-H groups, was
338 common to the spectrum of CSP, extracted and commercial celluloses (Fig. 7). However, the
339 peak was relatively broader for CSP, which was suggestive of the higher number of OH groups
340 due to its higher moisture content. In the spectrum of extracted cellulose, the peaks at 2900 and
341 1651 cm^{-1} wavenumbers were attributed respectively to the asymmetric stretching of C-H groups
342 and stretching of O-H groups, representing adsorbed water (Shen, Ghasemlou & Kamdem,
343 2015), while the peak at 1431 cm^{-1} was assigned to the bending of CH_2 groups of cellulose.
344 Similarly, the peaks at 1375, 1320, 1058, 1157 and 1032 cm^{-1} reflected the C-H_2 deformation
345 vibration, C-H_2 rocking vibration, C-O-C pyranose ring skeletal vibration, C-O-C asymmetric
346 valance vibration and C-O stretching vibration, respectively. The peak at 896 cm^{-1} is the
347 characteristic of the β-(1→4) linked glycosidic bonds in cellulose. The typical peaks related to
348 lignin and hemicellulose were absent in the extracted cellulose.

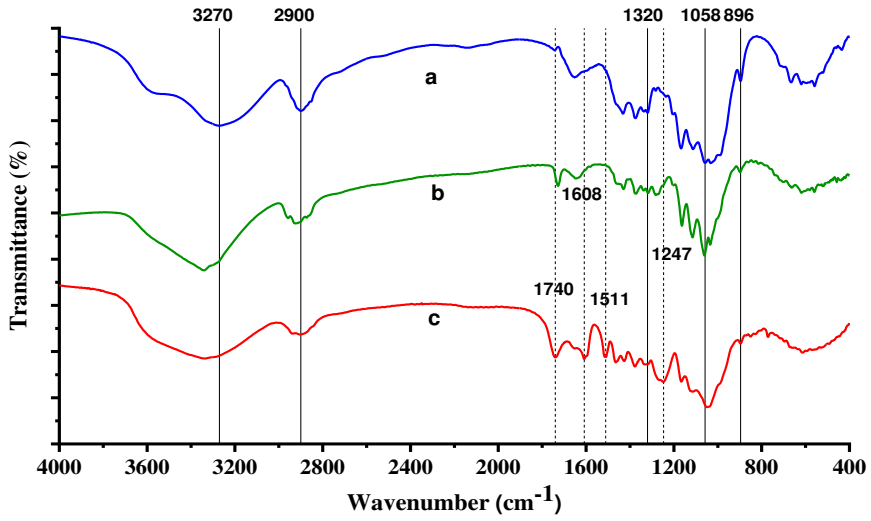

Fig. 7 Fourier transform infrared spectra (400 to 4000 cm^{-1} wavenumber) of (a) extracted cellulose (b) commercial cellulose and (c) coconut shell powder

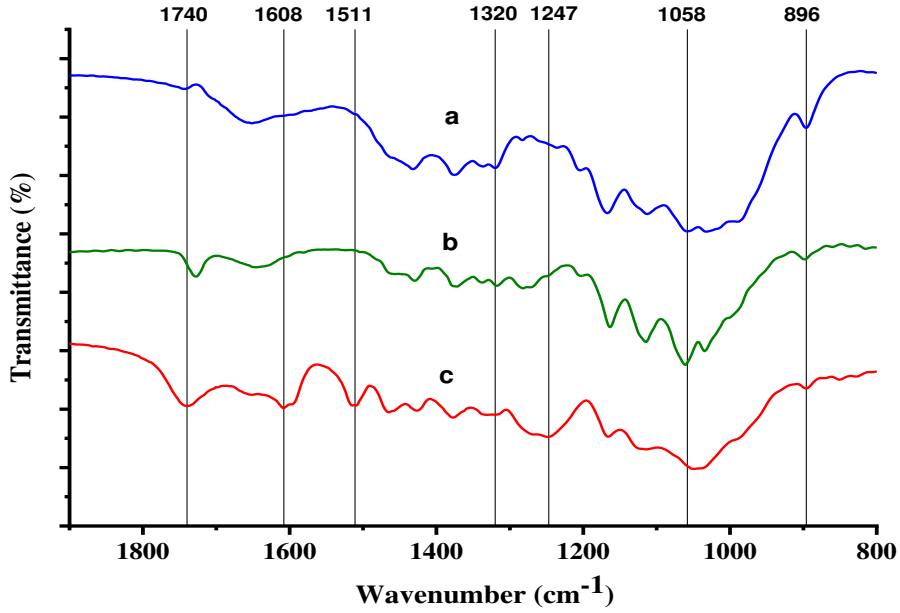

Fig. 8 Fourier transform infrared spectra (800 to 1900 cm^{-1} wavenumber) of (a) extracted cellulose (b) commercial cellulose and (c) coconut shell powder

359 **Table 1** Vibrational frequencies (cm^{-1}) of coconut shell powder and cellulose

Wavenumber (cm^{-1})	Coconut shell powder	Cellulose isolated from coconut shell powder and commercial cellulose
3400-3100	Stretching and bending bands of O-H groups in cellulose	Stretching and bending bands of O-H groups in cellulose
2900	-	Stretching of C-H groups
1740	C-O stretching of the acetyl and uronic ester groups of hemicellulose	Not present
1608	Indicates presence of lignin	Not present
1651	-	Stretching of O-H groups representing the adsorbed water in carbohydrate
1511	C=C stretching vibration in the aromatic ring of lignin	Not present
1431	-	Bending of CH_2 groups representing presence of cellulose in carbohydrate
1320	-	C-H_2 rocking vibration
1247	Presence of lignin and represents the C-O out of plane stretching vibration of the aryl group	Not present
1058	-	C-O-C pyranose ring skeletal vibration
896	-	C-H deformation vibration

360

361 *3.8. True density*

362 The true density of CSP, extracted and commercial cellulose was 1657, 1313 and 1470
363 kg/m^3, respectively. The true density of isolated cellulose was lower as compared to that of CSP
364 and commercial cellulose due to the increased voids created by separation of fibrillar bundles
365 into individual fibers during removal of lignin and hemicellulose. The alpha and beta

polymorphs of crystalline cellulose have true density of 1582 and 1599 kg/m^3, respectively (Sun, 2005). The closer the true density of cellulose to its crystalline counterpart, the higher is its degree of crystallinity (Achor, Oyeniyi, & Yahaya, 2014).

3.9. Flow properties

The flow properties of CSP and celluloses are summarized in Table 2. The bulk and tapped densities for cellulose were in accordance with those reported for lignocellulosic fibers from peanut husk (310 and 370 kg/m^3) (Azubuike, Odulaja, & Okhamafe, 2012). The bulk and tapped densities of extracted cellulose were higher than that of commercial cellulose but lower than the values of CSP. This might be due to the smaller particle size and less interparticle attractions due to its lower moisture content as compared to commercial cellulose. As moisture in commercial cellulose was higher (3.7% as compared to 2.5% for extracted cellulose), it promoted adhesion and liquid bridging between particles, leading to reduction in bulk density. In general, flowability of a material is better if the difference between bulk and tapped densities is lower. Thus, extracted cellulose had better flow characteristics than commercial cellulose because of less interparticular adhesion and bridging interactions due to lower moisture content. Particles having low internal porosity tend to possess better flow properties. As the porosity of cellulose extracted from CSP was lower (0.71) than that of cellulose (0.79), it was expected to have better flow properties as compared to commercial cellulose.

CI of greater than 25% for CSP and celluloses suggested that they were cohesive powders with ‘passable’ to ‘poor’ flowability (Wu, Ho, & Sheu, 2001). Amongst the three samples, the HR and CI of commercial cellulose were found to be higher than that of isolated cellulose. This could be ascribed to its higher moisture content, causing difficulties to flow due to adhesion and

390 bridging. The HR and CI data of commercial cellulose were supported by its higher value of
391 AoR as well. AoR, a qualitative indicator of cohesive and internal friction in the powders, is
392 presented in Table 1. In comparison to commercial grade, extracted cellulose had intermediate
393 cohesiveness and fair level of flowability. The AoR of CSP and extracted cellulose were slightly
394 above 40º, while that of commercial cellulose was 55.75º. The AoR of extracted cellulose lied
395 between the theoretical minimum of 20º for uniform spheres that flow very well and the
396 maximum of 45º for powders that flow poorly (Fowler, 2000).

397 **Table 2** Flow properties of coconut shell powder, extracted cellulose and commercial cellulose

Property	Sample		
	Coconut shell powder	Extracted cellulose	Commercial cellulose
Bulk density, kg/m^3	500.90±8.12	368.80±3.83	303.90±12.85
Tapped density, kg/m^3	682.50±6.17	493.80±4.16	452.30±3.42
True density, kg/m^3	1657.00±2	1313.00±1	1470.00±1
Hausner ratio	1.36±0.009	1.34±0.004	1.49±0.068
Carr's index (%)	26.61±0.532	25.30±0.262	32.80±3.116
Porosity	0.69±0.004	0.71±0.002	0.79±0.008
Angle of repose (deg)	43.17±0.017	44.18±0.026	55.75±0.150

398

399 *3.10. Reinforcing ability of cellulose fibers*

400 The thicknesses of casein and casein composite films were 0.224 and 0.282 mm,
401 respectively. The thickness of composite films increased with increase in cellulose content owing
402 to the larger particle size of cellulose. These results were in agreement with those of El Halal et
403 al. (2015) who reported that increase in addition of cellulose fiber extracted from barley husk
404 increased the thickness of barley grain starch films. Qazanfarzadeh and Kadivar (2016) also
405 reported increase in film thickness with increase in the proportion of oat nanocellulose fiber in
406 whey protein isolate (WPI) films.

407

408 The WVP and tensile properties of casein and casein composite films are summarized in
409 Table 3. The WVP of casein and casein composite films was 7.7×10^{-10} g/m.s.Pa and 11.6×10^{-10}
410 g/m.s.Pa, respectively. The WVP is affected d by the hydrophilic or hydrophobic nature of
411 materials, film manufacturing process, the type, amount and distribution of additives applied,
412 presence of voids and cracks, and final arrangement in polymer structure. The increase in WVP
413 of composite films could be due to the rough surface of cellulose, which might have caused
414 minor cracks or discontinuities in the casein network of the film (Abdulkhani, Hosseinzadeh,
415 Ashori, Dadashi, & Takzare, 2014). With increase in addition of cellulose, the film
416 microstructure changed, while the non-reinforced films exhibited smooth and homogeneous
417 structure. The increase in WVP with addition of cellulose could be due to the strong affinity to
418 materials containing hydroxyls (water), which led to swelling of cellulose at higher relative
419 humidity and causing disruption of structural network in the films (Pereda, Amica, Rácz, &
420 Marcovich, 2011). Abdulkhani et al. (2014) also reported similarly that addition of nanocellulose
421 fibers to polylactic acid film effected increase in WVP.
422
423 The tensile strength and Young's modulus of casein film were 4.98 and 9.91 MPa,
424 respectively, which increased to 7.20 and 83.42 MPa for casein composite films containing
425 extracted cellulose. The improvement in mechanical properties after addition of cellulose was
426 due to good dispersion and interactions between casein and cellulose vide strong hydrogen
427 bonds. The elongation at break of casein film was 52.08%, whereas it decreased to 8.66% for
428 casein composite films containing 3% cellulose presumably due to the rigidity of cellulose fibers.
429 Thus, casein composite films containing extracted cellulose were stiffer and harder. The results
430 of film properties were in accordance with those of corn starch-based composites (Haafiz et al.,

2013), WPI/nanocellulose films (Qazanfarzadeh & Kadivar, 2016) and microcrystalline cellulose-reinforced tamarind seed starch films (Sudharsan et al., 2016).

4. Conclusions

The process to extract cellulose from CSP by chemical treatment was standardized. The optical and SEM images of extracted cellulose showed a drastic reduction in fiber diameter as compared to CSP because the composite fibril structure was broken into individual cellulose micro-fibrils after removal of lignin and hemicellulose. The absence of lignin and hemicellulose in extracted cellulose was confirmed from FTIR spectra and XRD diffractograms. The extracted cellulose had crystallinity index of 65.9%, and had intermediate cohesiveness and better flowability as compared to commercial cellulose. Incorporation of cellulose as reinforcing fibers in casein improved the mechanical properties of the composite films considerably. From the tensile strength and Young's modulus data, it could be concluded that cellulose isolated from CSP had the potential as reinforcement fiber for the production of composite films. Application of composite films for food packaging helps to realize the potential of agricultural wastes as biopolymers and reduce pollution.

Acknowledgements

The authors thank the Director, ICAR-National Dairy Research Institute for the financial support. The authors are also grateful to CeNSE, Indian Institute of Science, Bengaluru for their technical assistance for major analytical tests of the samples.

Conflict of Interest

The authors declare no potential conflict of interest in this work.

References

Abdulkhani, A., Hosseinzadeh, J., Ashori, A., Dadashi, S., & Takzare, Z. (2014). Preparation and characterization of modified cellulose nanofibers reinforced polylactic acid nanocomposite. *Polymer Testing*, *35*, 73-79. https://doi.org/10.1016/j.polymertesting.2014.03.002

Achor, M., Oyeniyi, Y. J., & Yahaya, A. (2014). Extraction and characterization of microcrystalline cellulose obtained from the back of the fruit of *Lageriana siceraria* (water gourd). *Journal of Applied Pharmaceutical Science, 4*(1), 57-60. https://doi.org/10.7324/JAPS.2014.40109.

ASTM D1103-60 (1977) Method of test for alpha-cellulose in wood, American Society for Testing and Materials, USA.

ASTM D1104-56 (1978) Method of test for holocellulose in wood, American Society for Testing and Materials, USA.

ASTM E96-95. (1995). Standard test methods for water vapour transmission of materials, American Society for Testing and Materials, USA.

Azubuike, C. P., Odulaja, J., & Okhamafe, A. O. (2012). Physicotechnical, spectroscopic and thermogravimetric properties of powdered cellulose and microcrystalline cellulose derived from groundnut shells. *Journal of Excipients and Food Chemistry, 3* (3), 106-115.

Bodirlau, R., Teaca, C.A., & Spiridon, I. (2013). Influence of natural fillers on the properties of starch-based biocomposite films. *Composites Part B: Engineering, 44*(1), 575-583. https://doi.org/10.1016/j.compositesb.2012.02.039

Bonnaillie, L. M., Zhang, H., Akkurt, S., Yam, K. L., & Tomasula, P. M. (2014). Casein films: The effects of formulation, environmental conditions and the addition of citric pectin on the structure and mechanical properties. *Polymers*, *6*(7), 2018-2036. https://doi.org/10.3390/polym6072018.

Collazo-Bigliardi, S., Ortega-Toro, R., & Boix, A.C. (2018) Isolation and characterisation of microcrystalline cellulose and cellulose nanocrystals from coffee husk and comparative study with rice husk. *Carbohydrate Polymers*, *191,* 205-215. https://doi.org/10.1016/j.carbpol.2018.03.022.

Deepa, B., Abraham, E., Cherian, B.M., Bismarck, A., Blaker, J.J., Pothan, L.A., Leao, A.L., De Souza, S.F., & Kottaisamy, M. (2011). Structure, morphology and thermal characteristics of banana nano fibers obtained by steam explosion. *Bioresource Technology, 102*(2), 1988-1997. https://doi.org/10.1016/j.biortech.2010.09.030.

Deka, H., Misra, M., & Mohanty, A. (2013). Renewable resource based "all green composites" from kenaf biofiber and poly (furfuryl alcohol) bioresin. *Industrial Crops and Products*, *41*, 94-101. https://doi.org/10.1016/j.indcrop.2012.03.037.

Dufresne, A., & Vignon, M. R. (1998). Improvement of starch films performances using cellulose microfibrils. *Macromolecules*, *31*(8), 2693-2696. https://doi.org/10.1021/ma971532b.

El Halal, S. L. M., Colussi, R., Deon, V. G., Pinto, V. Z., Villanova, F. A., Carreño, N. L. V., Dias, A.R.G., & da Rosa Zavareze, E. (2015). Films based on oxidized starch and cellulose from barley. *Carbohydrate Polymers*, *133*, 644-653. https://doi.org/10.1016/j.carbpol.2015.07.024.

Fowler, H.W. (2000). Powder flow and compaction. In C.J.S. Carter (Ed), *Cooper and Gunn's tutorial pharmacy* (pp 211-233).

Gassan, J., & Bledzki, A. K. (1999). Possibilities for improving the mechanical properties of jute/epoxy composites by alkali treatment of fibres. *Composites Science and Technology*, *59*(9), 1303-1309. https://doi.org/10.1016/S0266-3538(98)00169-9.

Haafiz, M. M., Hassan, A., Zakaria, Z., Inuwa, I. M., Islam, M. S., & Jawaid, M. (2013). Properties of polylactic acid composites reinforced with oil palm biomass microcrystalline cellulose. *Carbohydrate Polymers*, *98*(1), 139-145. https://doi.org/10.1016/j.compositesb.2012.02.039.

Hahary, F. N., Husseinsyah, S., & Zakaria, M. M. (2016). Improved properties of coconut shell regenerated cellulose biocomposite films using butyl methacrylate. *BioResources*, *11*(1), 886-898. https://doi.org/10.15376/biores.11.1.886-898.

Ilyas, R. A., Sapuan, S. M., Ishak, M. R., & Zainudin, E. S. (2017). Effect of delignification on the physical, thermal, chemical, and structural properties of sugar palm fibre. *BioResources*, *12*(4), 8734-8754. https://doi.org/10.15376/biores.12.4.8734-8754.

John, M. J., & Anandjiwala, R. D. (2008). Recent developments in chemical modification and characterization of natural fiber-reinforced composites. *Polymer Composites*, *29*(2), 187-207.https://doi.org/10.1002/pc.20461.

Jumaidin, R., Sapuan, S. M., Jawaid, M., Ishak, M. R., & Sahari, J. (2017). Effect of seaweed on mechanical, thermal, and biodegradation properties of thermoplastic sugar palm starch/agar composites. *International Journal of Biological Macromolecules*, *99*, 265-273.https://doi.org/10.1016/j.ijbiomac.2017.02.092.

Liyanage, C. D., & Pieris, M. (2015). A physico-chemical analysis of coconut shell powder. *Procedia Chemistry*, *16*, 222-228. https://doi.org/10.1016/j.proche.2015.12.045.

Madakson, P. B., Yawas, D. S., & Apasi, A. (2012). Characterization of coconut shell ash for potential utilization in metal matrix composites for automotive applications. *International Journal of Engineering Science and Technology*, *4*(3), 1190-1198.

Majeed, K., Jawaid, M., Hassan, A. A. B. A. A., Bakar, A. A., Khalil, H. A., Salema, A. A., & Inuwa, I. (2013). Potential materials for food packaging from nanoclay/natural fibres filled hybrid composites. *Materials & Design*, *46*, 391-410.. https://doi.org/10.1016/j.matdes.2012.10.044.

Mantia, F. P. L., Morreale, M., & Ishak, Z. M. (2005). Processing and mechanical properties of organic filler–polypropylene composites. *Journal of Applied Polymer Science, 96*(5), 1906-1913. https://doi.org/10.1002/app.21623.

McHugh, T.H., & J.M. Krochta. (1994). Milk-protein-based edible films and coatings. *Food Technology, 48, 97–103.*

Mitra, H., Pushpadass, H. A., Franklin, M. E. E., Ambrose, R. K., Ghoroi, C., & Battula, S. N. (2017). Influence of moisture content on the flow properties of basundi mix. *Powder Technology*, *312*, 133-143. https://doi.org/10.1016/j.powtec.2017.02.039.

Pereda, M., Amica, G., Rácz, I., & Marcovich, N. E. (2011). Structure and properties of nanocomposite films based on sodium caseinate and nanocellulose fibers. *Journal of Food Engineering, 103*(1), 76-83. http://dx.doi.org/10.1016/j.jfoodeng.2010.10.001.

Pushpadass, H. A., Emerald, F. M. E., Rao, K. J., Nath, B. S., & Chaturvedi, B. (2014). Prediction of shelf life of gulabjamun mix using simulation and mathematical modeling–based on moisture gain. *Journal of Food Processing and Preservation*, *38*(4), 1517-1526. https://doi.org/10.1111/jfpp.12111.

Qazanfarzadeh, Z., & Kadivar, M. (2016). Properties of whey protein isolate nanocomposite films reinforced with nanocellulose isolated from oat husk. *International Journal of Biological Macromolecules*, *91*, 1134-1140. https://doi.org/10.1016/j.ijbiomac.2016.06.077.

Razali, N., Salit, M. S., Jawaid, M., Ishak, M. R., & Lazim, Y. (2015). A study on chemical composition, physical, tensile, morphological, and thermal properties of roselle fibre: Effect of fibre maturity. *BioResources*, *10*(1), 1803-1824. https://doi.org/10.15376/biores.10.1.1803-1824.

Sarki, J., Hassan, S. B., Aigbodion, V. S., & Oghenevweta, J. E. (2011). Potential of using coconut shell particle fillers in eco-composite materials. *Journal of Alloys and Compounds*, *509*(5), 2381-2385.https://doi.org/10.1016/j.jallcom.2010.11.025.

Satyanarayana, K. G., Arizaga, G. G., & Wypych, F. (2009). Biodegradable composites based on lignocellulosic fibers—An overview. *Progress in polymer science*, *34*(9), 982-1021. https://doi.org/10.1016/j.progpolymsci.2008.12.002.

Segal, L. G. J. M. A., Creely, J. J., Martin Jr, A. E., & Conrad, C. M. (1959). An empirical method for estimating the degree of crystallinity of native cellulose using the X-ray diffractometer. *Textile Research Journal*, *29*(10), 786-794. https://doi.org/10.1177/004051755902901003.

Shen, Z., Ghasemlou, M., & Kamdem, D. P. (2015). Development and compatibility assessment of new composite film based on sugar beet pulp and polyvinyl alcohol intended for packaging applications. *Journal of Applied Polymer Science*, *132*(4), 41354. https://doi.org/10.1002/app.41354.

Singha, A. S., & Thakur, V. K. (2009). Morphological, thermal, and physicochemical characterization of surface modified pinus fibers. *International Journal of Polymer Analysis and Characterization*, *14*(3), 271-289. https://doi.org/10.1080/10236660802666160.

Sofla, M. R. K., Brown, R. J., Tsuzuki, T., & Rainey, T. J. (2016). A comparison of cellulose nanocrystals and cellulose nanofibres extracted from bagasse using acid and ball milling methods. *Advances in Natural Sciences: Nanoscience and Nanotechnology*, *7*(3), 035004. http://dx.doi.org/10.1088/2043-6262/7/3/035004.

Sonia, A., & Dasan, K. P. (2014). Barrier properties of celluloses microfibers (CMF)/ethylene-co-vinyl acetate (EVA)/composites. *Composite Interfaces*, *21*(3), 233-250. https://doi.org/10.1080/15685543.2014.856644.

Sudharsan, K., Mohan, C. C., Babu, P. A. S., Archana, G., Sabina, K., Sivarajan, M., & Sukumar, M. (2016). Production and characterization of cellulose reinforced starch (CRT) films. *International Journal of Biological Macromolecules*, *83*, 385-395. https://doi.org/10.1016/j.ijbiomac.2015.11.037.

Sun, C. C. (2005). True density of microcrystalline cellulose. *Journal of Pharmaceutical Sciences*, *94*(10), 2132-2134. https://doi.org/10.1002/jps.20459.

Tawakkal, I. S. M., Talib, R. A., Abdan, K., & Ling, C. N. (2012). Mechanical and physical properties of kenaf-derived cellulose (KDC)-filled polylactic acid (PLA) composites. *BioResources*, *7*(2), 1643-1655. http://doi.org/10.15376/BIORES.7.2.1643-1655.

Teacă, C. A., Bodîrlău, R., & Spiridon, I. (2013). Effect of cellulose reinforcement on the properties of organic acid modified starch microparticles/plasticized starch bio-composite films. *Carbohydrate polymers*, *93*(1), 307-315. https://doi.org/10.1016/j.carbpol.2012.10.020.

Thakur, V. K., Thakur, M. K., & Gupta, R. K. (2014). Raw natural fiber–based polymer composites. *International Journal of Polymer Analysis and Characterization*, *19*(3), 256-271.. https://doi.org/10.1080/1023666X.2014.880016.

Wagh, Y. R., Pushpadass, H. A., Emerald, F., & Nath, B. S. (2014). Preparation and characterization of milk protein films and their application for packaging of Cheddar cheese. *Journal of Food Science and Technology*, *51*(12), 3767-3775. https://doi.org/10.1007/s13197-012-0916-4.

Wu, J. S., Ho, H. O., & Sheu, M. T. (2001). A statistical design to evaluate the influence of manufacturing factors on the material properties and functionalities of microcrystalline cellulose. *European Journal of Pharmaceutical Sciences*, *12*(4), 417-425. https://doi.org/10.1016/S0928-0987(00)00196-2.

Statements and Declarations

Funding

The authors declare that no funds, grants, or other support were received during the preparation of this manuscript.

Competing Interests

The authors have no relevant financial or non-financial interests to disclose.

Author Contributions

All authors contributed to the study conception and design. Material preparation, data collection and analysis were performed by Adarsh M. Kalla, Magdaline Eljeeva Emerald Franklin, Heartwin A. Pushpadassa, Sathish Kumar M.H. and Surendra Nath Battulaa. The first draft of the manuscript was written by Adarsh M. Kalla and all authors commented on previous versions of the manuscript. All authors read and approved the final manuscript.

Data Availability

The datasets generated during and/or analysed during the current study are available from the corresponding author on reasonable request.